JOURNAL OF SOLID STATE CHEMISTRY 110, 234–242 (1994)

Single Crystal Structure, Magnetic Properties, and Electronic Structure of $Tl_xCr_5S_8$ (x = 1.0 and 0.7)

W. Bensch and E. Wörner

Institute for Inorganic Chemistry, University of Frankfurt, Niederurseler Hang, 60439 Frankfurt am Main, Germany

M. Muhler

Fritz Haber Institut, Faradayweg 4, 14195 Berlin, Germany

and

U. Ruschewitz

Institute for Inorganic Chemistry, RWTH Aachen, Prof.-Pirlet-Str. 1, 52074 Aachen, Germany

Received February 15, 1993; in revised form September 14, 1993; accepted September 15, 1993

$TlCr_5S_8$ is isotypic with TlV_5S_8. It consists of layers of edge sharing CrS_6-octahedra connected by other CrS_6-octahedra to a three-dimensional network. The distances within the two-dimensional metal atom network are irregularly distributed with one short (2.959 Å) and two longer (3.332 and 3.339 Å) separations between neighboring Cr atoms. The environment of the Tl atoms within the rectangular channels is highly asymmetric and may be described as a 4 + 6 coordination. Magnetic susceptibility measurements show maxima of the susceptibility at about 125 and 145 K for the Tl-rich and Tl-poor samples, respectively. The shape of the susceptibility maxima is atypical and points to a complex interaction of the magnetic moments. Ultraviolet photoelectron spectroscopy (UPS) reveals that $TlCr_5S_8$ is a semiconductor. The valence band is composed of S 3*p* and Cr 3*d* states with a broadening due to the hybridization with Tl 6*s* and 6*p* states. The Tl atoms as well as the Cr atoms carry a low formal positive charge and the interactions between the guest Tl and the Cr_5S_8 host matrix are highly covalent.

1. INTRODUCTION

After the pioneering preparation of the ternary compound TlV_5S_8 (1), a number of isotypic compounds with the formal composition $A_xM_5X_8$ (A = K, Cs, Rb, In, Tl; M = Ti, V, Cr; X = S, Se) (2–11) have been prepared. Magnetic data of "$TlCr_5S_8$" have been published (12), but the reported lattice parameters of this compound are remarkably different from those reported in Ref. (8) and obtained during our work. They cannot be transformed into the cell of $TlCr_5S_8$ by a standard reduction algorithm.

The present contribution reports the single crystal structure of $TlCr_5S_8$. The properties were investigated with respect to the magnetic behavior and electronic structure to get insight into the interaction between the guest atom Tl and the host lattice Cr_5S_8. Unfortunately, single crystals with a Tl content of 0.7 were not available.

2. EXPERIMENTAL

$TlCr_5S_8$ was prepared by reacting the elements in evacuated and sealed silica ampoules. First, the mixture was heated to 1273 K with a heating rate of 100 K/hr and held at this temperature for 10 days. After reducing the temperature to 1223 K, the tube was fired for 5 days. Finally, the mixture was cooled to room temperature with a cooling rate of 50 K/hr. The product consisted of microcrystalline black powder, some small black needles, and tiny platelet-shaped crystals. The X-ray powder pattern was successfully indexed on the basis of the monoclinic $TlCr_5S_8$ structure.

A sample with the composition $Tl_{0.7}Cr_5S_8$ was prepared with a chemical redox reaction using 1 mg Br_2 in 1 ml CH_3CN (13). After a 210-hr reaction time, the final composition was reached. Single crystals with a Tl content significantly lower than x = 0.7 in $Tl_xCr_5S_8$ could not be prepared in this way. Atomic absorption spectroscopy (AAS) was carried out to determine the Tl abundance in the reaction product. The homogeneity of the sample was checked using X-ray powder diffractometry.

A needle-shaped single crystal with the composition $TlCr_5S_8$ with approximate dimensions 0.05 × 0.1 × 0.05 mm^3 was used for the data collection on a STOE AED II diffractometer (MoK_α, λ = 0.71073 Å). Intensities were collected at 295 K. The data were corrected for Lorentz, polarization effects and a numerical absorption correction

0022-4596/94 $6.00

was applied. Anomalous dispersion correction was taken into account. Some technical details as well as refinement results are summarized in Table 1. In Table 2 atomic coordinates and equivalent displacement coefficients U_{eq} are listed. All calculations were performed in the space group $C2/m$ with the program package SHELXTL Plus.

The susceptibility measurements were performed between 4.2 and 300 K with a Faraday balance at various fields up to 1.406 T. Some technical characteristics of the gauge have been described (14). The small field dependence of the measured susceptibilities which was due to ferromagnetic impurities was eliminated by a Honda–Owen plot. The magnetic data were fitted with the program CURIE. X-ray photoelectron spectroscopy (XPS, MgK_α = 1253.6 eV) and ultraviolet photoelectron spectroscopy (UPS, He I = 21.2 eV, He II = 40.8 eV) were carried out in a Leybold Heraeus LH 200 system. The base pressure of the apparatus was 2×10^{-10} Torr. The energy scale was calibrated using Au $4f_{7/2}$ = 84.0 eV. The spectra are shown as untreated raw data (dots) and after smoothing (solid lines). The quantitative results were obtained after Shirley background subtraction and integration using the empirically derived cross sections of Ref. (15). The $TlCr_5S_8$ sample was transferred into the preparation chamber (base pressure 1×10^{-9} mbar) as loose powder in a mortar-like stainless steel sample holder. A wobble stick (VG Instruments) equipped with a stainless steel pestle was used to grind the sample in UHV.

TABLE 1
Technical Details and Refinement Results for $TlCr_5S_8$ (Single Crystal) and $Tl_{0.7}Cr_5S_8$

$TlCr_5S_8$	Single crystal	Ref. (8)	$Tl_{0.7}Cr_5S_8$[a]
a[Å]	17.803(4)	17.767(6)	17.716(2)
b[Å]	3.436(1)	3.431(1)	3.4165(3)
c[Å]	8.589(3)	8.594(3)	8.585(1)
β[°]	104.65(3)	104.68(3)	104.33(1)
a/b	5.181	5.178	5.185
c/a	0.482	0.484	0.485
V[Å^3]	508.3(2)	506.78	503.49(7)
d_{calc} [g/cm^3]	4.710		
μ [mm^{-1}]	22.53		
N_0 [>4 $\sigma(F)$]	572		
N_p	46		
x[b]	0.0007(1)		
y[c]	0.0001		
δ [e/Å^3]	2.93		
	−1.88		
R [%]	3.95		
R_w [%]	4.40		
GOOF	1.36		
Tl U_{11}/U_{22}	3.93		
Tl U_{11}/U_{33}	2.37		
Tl U_{22}/U_{33}	0.60		

[a] Refined from X-ray powder data.
[b] Extinction coefficient in $F^* = F\,[1 + 0.002\,F^2\,x/\sin 2\Theta]^{-1/4}$.
[c] y in weighting scheme $w = 1/(\sigma^2(F) + y\,F^2)$.

TABLE 2
Atomic Coordinates (× 10^4) and Equivalent Isotropic Displacement Coefficients (Å^2 × 10^3)

Atom	x	y	z	U_{eq}
Tl	0	0	0	49(1)
Cr(1)	0	5000	5000	9(1)
Cr(2)	7947(1)	0	1640(2)	9(1)
Cr(3)	1577(1)	0	4801(2)	9(1)
S(1)	6687(1)	0	−89(3)	9(1)
S(2)	5852(1)	0	3245(3)	10(1)
S(3)	2606(1)	0	3427(3)	8(1)
S(4)	9247(1)	0	3431(3)	8(1)

[a] The equivalent isotropic displacement coefficient is defined as one third of the trace of the orthogonalized U_{ij} tensor.

3. RESULTS AND DISCUSSION

3.1. The Crystal Structure

A plot of the crystal structure is shown in Fig. 1. The insertion depicts the tenfold coordination of the Tl atoms. The structure can be described as a three-dimensional framework of MS_6 octahedra sharing edges and faces. Infinite layers of $M(1)$ and $M(3)$ octahedra sharing edges are parallel to (001) and infinite double units made up of $M(2)$ octahedra with common edges are along the b-axis. The double units connect the layers via common faces. The electropositive element A is confined within the rectangular channels. Important interatomic distances are given in Table 3. The lattice parameters are in good agreement with those obtained from the refinement of X-ray powder data (8).

The anisotropic displacement parameter (ADP) U_{11} of the Tl atom is significantly larger than the other U_{ii} components, suggesting a displacement of the Tl atoms from the center of the tenfold coordination polyhedron toward the $Cr(1)S_6$ double unit (see Table 1). The ADPs of the other atoms behave as expected. It is noted that in TlV_5S_8, the U_{22} of Tl is significantly larger than the other U_{ii} components, pointing to a different kind of displacement (16).

The average Tl–S bond distance, as well as the difference δ between the largest and shortest Tl–S separation, which is an indication for the asymmetry of the environment of the Tl atoms, is clearly larger than in the isotypic compounds $Tl_{0.92}V_5S_8$ (16) and $TlTi_5S_8$ (8). The Tl–S distances can be divided into two groups (see Table 3). The Tl–S2 distance is shorter than the sum of the ionic radii (Tl^+, 1.65 Å, S^{2-}, 1.84 Å), indicating covalent bonding interactions. The Tl–S separations of the other group (Tl–S1, Tl–S4) are nearly identical to the sum of the ionic

radii. Therefore, the environment around Tl is best described by a 4 + 6 coordination.

The octahedra around Cr2 and Cr3 are more distorted than the Cr1 octahedron (see Table 3). The average Cr–S distances are of the order observed in binary and ternary Cr sulfides.

The arrangement of the Cr atoms is schematically displayed in Fig. 2. The connection of the $Cr(2)S_6$ and $Cr(3)S_6$ octrahedra via common faces leads to the formation of Cr2–Cr3 contacts of 2.959(2) Å which are about 16.5% larger than those in Cr metal, whereas the separations Cr1–Cr3 and Cr2–Cr2 are about 31% larger than those in Cr metal. Treating these Cr1–Cr3 and Cr2–Cr2 separations as weak Cr–Cr interactions the resulting metal atom net is composed of layers of infinite double zigzag chains of Cr1 and Cr3 atoms parallel to the (001) plane. Single zigzag chains of Cr2 atoms which are parallel to the *b*-axis connect these layers. The average Cr–Cr separation yields 3.281 Å.

Alternatively, if the Cr1–Cr3 and Cr2–Cr2 separations are regarded as noninteracting, the resulting Cr atom arrangement consists of isolated Cr_2-pairs (or Cr_2-dimers) of Cr2–Cr3 atoms and isolated Cr1 atoms.

3.2. Magnetic Susceptibility

The temperature dependence of the magnetic susceptibility of $TlCr_5S_8$ and $Tl_{0.7}Cr_5S_8$ is presented in Fig. 3. The susceptibility of $TlCr_5S_8$ passes a maximum at around 125 K; for $Tl_{0.7}Cr_5S_8$ a maximum occurs at 145 K. It was proposed that below a critical distance R_c of about 3.5 Å, direct interactions between Cr^{3+}–Cr^{3+} favor antiferromagnetic ordering, whereas indirect 90° Cr^{3+}–anion–Cr^{3+} interactions are ferromagnetic (17). In the title compound the Cr–Cr separations are below the critical value of 3.5 Å. Hence, direct as well as indirect interactions may be responsible for the observed susceptibility maxima.

The susceptibility vs temperature curve is indicative for a complex behavior which involves contributions from a low-dimensional magnetic system and contributions from a Curie–Weiss (C–W) magnet. Similar curves are observed for binuclear iron sulfides like Cs_3FeS_3 (18). It is noted that in these iron compounds the Fe_2S_6 double tetrahedra are isolated by the large alkali cations. As discussed in the previous section, the case of a one-dimensional Cr-chain as the low-dimensional magnetic system is rejected. The following model may, in part, be in accordance with the results of the crystal structure analysis. The Cr2–Cr3 atoms (CrS_6 octahedra with common faces) form Cr_2-dimers ($S = 3/2$) and are in an antiferromagnetic groundstate. The Curie–Weiss-like contribution comes from the Cr1 atom ($S = 3/2$) which only has Cr3 neighbors at a distance of 3.332 Å.

It is well documented that magnetic susceptibility data of binuclear complexes with spins greater than 1/2 are difficult to interpret (19). The spin Hamiltonian for $S = 3/2$ dimers is complicated by the addition of an *intraionic* spin coupling term (D) to the dimer exchange term (J) and an *interdimer* exchange interaction must also be taken into account. In the present analysis these additional terms are not considered. Furthermore, different variables are highly correlated and hence, values obtained from powder measurements should be viewed with caution.

The following equation was chosen (19) to fit the experimental data:

$$\chi = p[A \times ((2 \times e^{2x} + 10 \times e^{6x} + 28 \times e^{12x})/(1 + 3 \times e^{2x} + 5 \times e^{6x} + 7 \times e^{12x}))] + \chi(\mathrm{TIP}) + (1 - p) \times (C/T - \Theta). \quad [1]$$

$A = N \times g^2 \times \mu_B^2/k \times T$ and $x = J/k \times T$ (N is the Avogadro's constant, μ_B is the Bohr magneton, k is the Boltzmann constant, J is the exchange constant, C is the Curie constant and Θ is the Weiss constant). The variable p accounts for the dimer and C–W contributions. A value of 0.8 means that four of the five Cr atoms are present as dimers.

The results of the fitting procedure are summarized in Table 4 and are graphically displayed in Fig. 3 as dotted lines. As can be seen, the fits do not describe the experimental data in a fully satisfactory way. Analyzing the numerical values obtained by the fitting procedures, the following points must be stressed: for $TlCr_5S_8$, the variable p was fixed at 0.8; for $Tl_{0.7}Cr_5S_8$, such a high value yields an unrealistically high Curie constant. Consequently, the variable p was also refined and a reasonable value for the Curie constant was obtained for $p = 0.45$. The negative values for the TIP may be due to an inappropriate correction for the core diamagnetism.

The evaluated values for the Weiss constant Θ are indicative of stronger antiferromagnetic interaction in $Tl_{0.7}Cr_5S_8$ than in $TlCr_5S_8$. This is accordance with the larger value for the coupling constant J for the Tl-poor sample. It must be stressed here that it is not possible to separate intra- (within Cr_2-dimers) and interionic (between dimers) contributions to the coupling constant. The Tl-poor sample exhibits a lower value for p and larger values for J, Θ, and the Curie constant. Therefore, the exchange interactions in $Tl_{0.7}Cr_5S_8$ seem to be more pronounced than those in $TlCr_5S_8$. The contribution from the Cr_2-dimer to the total susceptibility is smaller and the larger Curie constant is indicative of more localized *d*-electron density in $Tl_{0.7}Cr_5S_8$. This interpretation is in line with structural arguments. In $Tl_xV_5S_8$, as well as in $Tl_xCr_5Se_8$, remarkable changes of the M–M interatomic distances are observed with decreasing Tl abundance (16, 20). Assuming similar changes for $Tl_xCr_5S_8$, the enlarge-

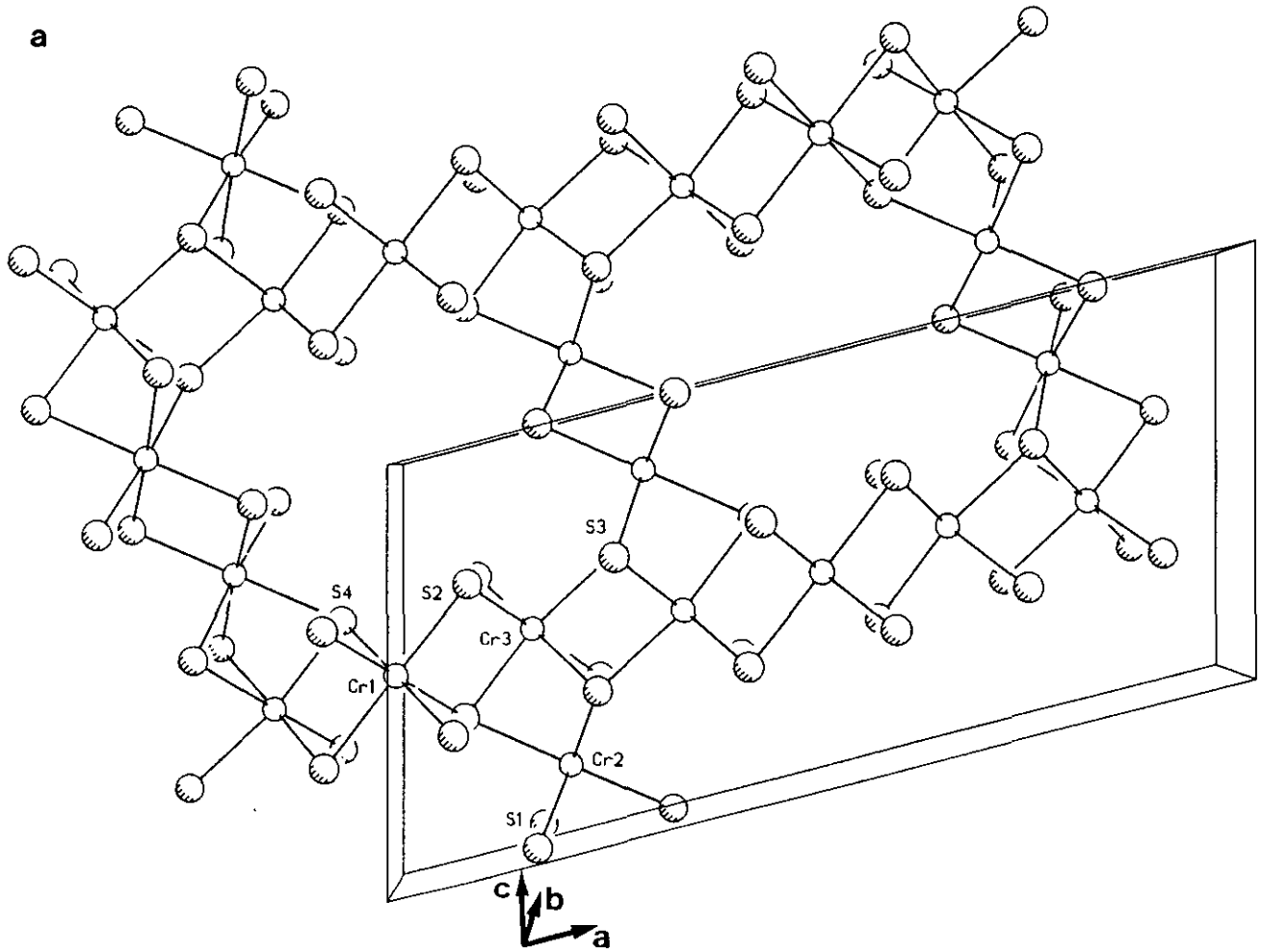

FIG. 1. (a) The crystal structure of $TlCr_5S_8$. The Tl atoms are located in the large channels. (b) The tenfold environment about the Tl atoms.

ment of the Cr2–Cr3 (Cr_2-dimer) distance is accompanied by a decrease of the Cr2–Cr2 and Cr1–Cr3 separations. Hence, the strength of the coupling constant *within* the dimers is lowered and the exchange interaction *between* the dimers and *between* Cr3 and Cr1 is enhanced, leading to a larger coupling constant J.

In addition, two further approaches were chosen to explain the susceptibility data. In the first attempt, the high temperature region (150–300 K and 185–300 K for $TlCr_5S_8$ and $Tl_{0.7}Cr_5S_8$, respectively) was fitted only with a C–W law. If the fit range is extended to lower temperatures, a comparable figure of merit for the fit is obtained with a temperature independent Pauli-paramagnetism (TIP) and a C–W contribution.

The magnetic moment μ_{exp} was calculated in the usual way. The μ_{exp} should be compared with the spin only moment of the Cr ions which were assumed to be in the valence state Cr^{3+} (d^3) (μ = 3.87 μ_B).

The evaluated magnetic data are listed in Table 4. Assuming a pure C–W behavior, the calculated magnetic moments for $TlCr_5S_8$ and $Tl_{0.7}Cr_5S_8$ are 5.64 μ_B/Cr and 4.04 μ_B/Cr, respectively. These values are larger than the expected μ_{eff} for Cr^{3+}. The values for the Weiss constant Θ of -1220 and -410 K for $TlCr_5S_8$ and $Tl_{0.7}Cr_5S_8$ are indicative for strong antiferromagnetic interactions between the local magnetic moments.

Completely different results are obtained assuming a TIP contribution to the magnetic susceptibilities. The value for μ_{exp} for $TlCr_5S_8$ of 1.21 μ_B/Cr is unrealistic low, whereas μ_{exp} for $Tl_{0.7}Cr_5S_8$ of 2.99 μ_B is of the order observed in other Cr chalcogenides (see Table 4). Again, the large negative values for Θ suggest strong antiferromagnetic interactions. It is noted that Θ is now more negative for $Tl_{0.7}Cr_5S_8$ than for $TlCr_5S_8$.

The TIP for both compounds is unusually high. Large values for the TIP are observed for metals or semiconductors with small conduction bands with a predominantly metal d character. But the UPS investigations of $TlCr_5S_8$ show no emission near E_F which could be attributed to Cr 3d states (see below). Therefore, the explanation of

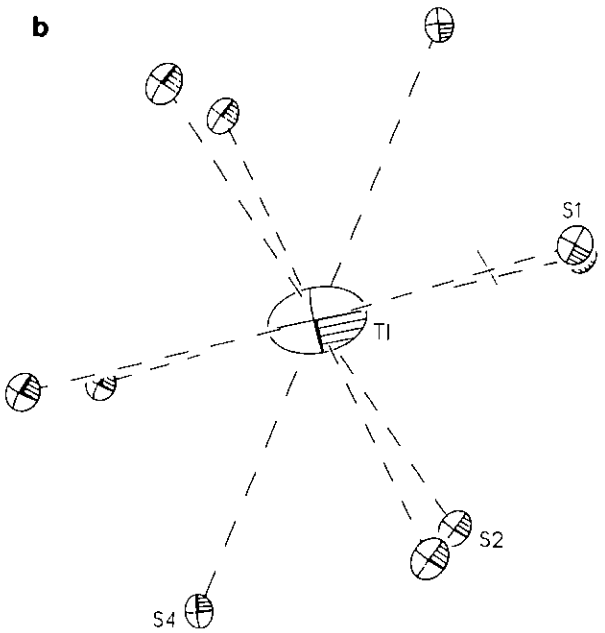

FIG. 1—*Continued*

the magnetic susceptibility with the coexistence of a C–W term and a TIP seems to be highly unlikely.

In summary, the different magnetic properties of $TlCr_5S_8$ and $Tl_{0.7}Cr_5S_8$ suggest significant differences of the interactions between the Cr atoms. But the magnetic models discussed above do not explain the observed behavior in a satisfactory way. Further investigations such as neutron scattering experiments are under way to clarify the magnetic properties of these compounds.

3.3. X-ray Photoelectron Spectroscopy (XPS)

Photoemission studies of air-sensitive materials prepared *ex situ* are rendered difficult by the transfer into ultrahigh vacuum (UHV) which usually makes a short exposure to air necessary. Cleaning procedures in UHV such as high temperature annealing or Argon ion sputtering are rarely applicable to ionic or covalent solids which would decompose under these conditions. In this study, the $TlCr_5S_8$ sample was ground in UHV in order to prepare fresh surfaces. Grinding had no effect on the measured binding energies. The surface composition was found to change from $Tl_{2.5}Cr_5S_{13.3}$ to $Tl_{1.3}Cr_5S_{6.5}$ after grinding, in good agreement with the nominal composition. Furthermore, grinding was found to be necessary to obtain UP spectra although no indication for charging was found with XPS.

The evaluated binding energies (b.e.) of the different core levels, as well as the b.e.'s of selected compounds, are summarized in Table 5.

3.3.1. The He I and He II UP spectra. The He I and He II UP spectra are displayed in Fig. 4. Both spectra exhibit no Fermi edge. Because no charging up effects are observed, the absence of a Fermi edge suggests that $TlCr_5S_8$ is a semimetal or a semiconductor with a small band gap between E_F and the valence band edge. The electrical resistivity measured on a pressed powder pellet yields 80 kΩ at 295 K. The resistivity increases with decreasing temperature, suggesting that $TlCr_5S_8$ is a semiconductor.

TABLE 3
Important Interatomic Distances in $TlCr_5S_8$

Tl–S1 4×	3.477(2)	Cr1–S2 2×	2.394(3)
–S2 4×	3.299(2)	–S4 4×	2.377(2)
Tl–S4 2×	3.532(3)	δ (Cr–$S_{max-min}$)	0.017
δ (Tl–$S_{max-min}$)	0.233	⟨Cr1–S⟩	2.383
⟨Tl–S⟩	3.417		
Cr2–S1	2.356(2)	Cr3–S3	2.418(3)
–S4	2.435(2)	–S4	2.363(3)
–S1 2×	2.365(2)	–S2 2×	2.352(2)
–S3 2×	2.479(2)	–S3 2×	2.503(2)
δ (Cr–$S_{max-min}$)	0.123	δ (Cr–$S_{max-min}$)	0.151
⟨Cr2–S⟩	2.413	⟨Cr3–S⟩	2.415
Cr1–Cr3 4×	3.332(2)		
Cr2–Cr2 2×	3.339(2)		
Cr2–Cr3	2.959(2)		

[a] Standard deviations of the last significant digit are given in parentheses.

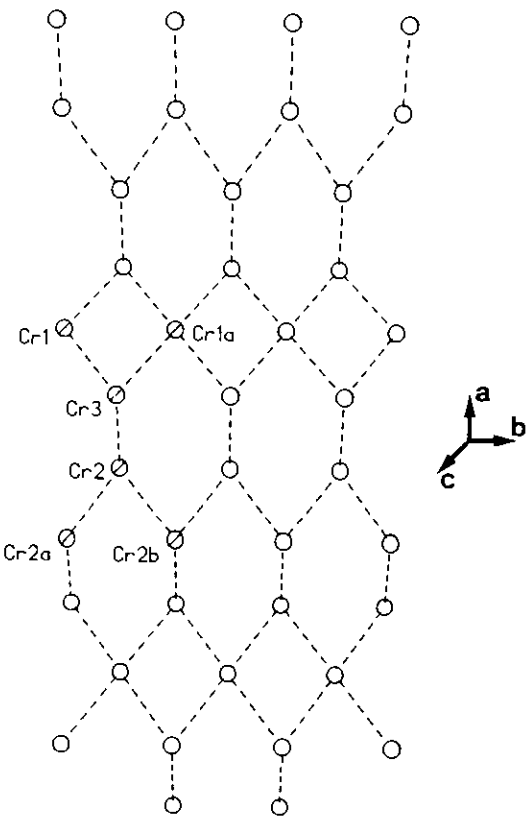

FIG. 2. The metal bonding pattern in $TlCr_5S_8$.

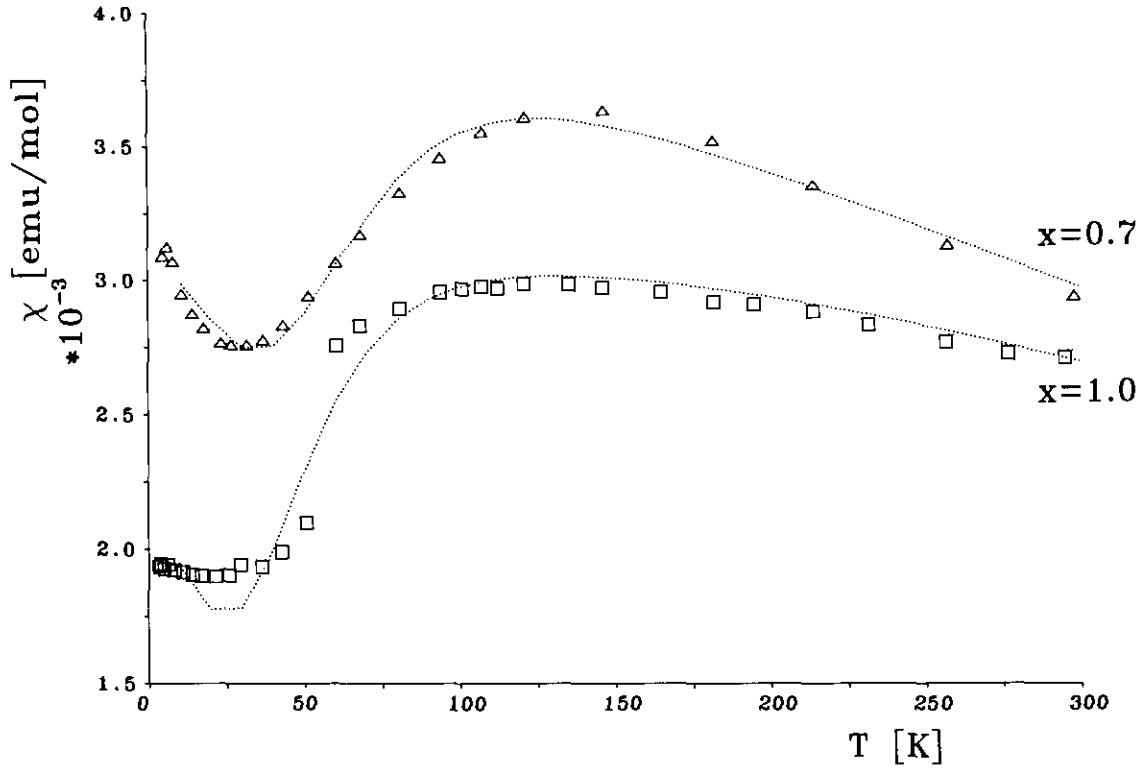

FIG. 3. The temperature dependence of the magnetic susceptibility of $TlCr_5S_8$ and $Tl_{0.7}Cr_5S_8$. The dotted lines represent the results of the fitting procedure using Eq. [1] (see text).

TABLE 4
Magnetic Data of $TlCr_5S_8$ and $Tl_{0.7}Cr_5S_8$[a]

Compound	T_c (K)	T_N (K)	χ_0 (10^{-6} emu/g)	Θ (K)	μ	Ref.
Cr_3S_4	—	220	—	−552	4.23	(27)
Cr_3Se_4	—	80	—	−48	4.7	(28)
Cr_3Te_4	319	—	—	—	—	(29)
Cr_5S_8	—	—	—	−688	4.05	(30)
Cr_5Se_8	—	—	—	−48	3.74	(30)
$TlCrS_2$	125(3)	—	—	120	3.59	(12)
$TlCrSe_2$	140	—	—	130	3.71	(12)
$TlCr_3S_5$	—	45	—	−259	3.43	(12)
$TlCr_3Se_5$	—	55	—	−156	2.79	(12)
Tl_3CrS_3	80	—	—	55	3.80	(12)
$In_xCr_5Se_8$	—	—	.72	−233	4.2	(5)
$Tl_xCr_5Te_8$	—	—	—	70	2.65	(5)
$K_xCr_5Se_8$	—	—	−2.2	−171	4.46	(5)
$Tl_xCr_5Se_8$	—	—	1.76	−218	4.01	(5)
$TlCr_5S_8$[b]	—	—	—	−1220	5.64	This work
$Tl_{0.7}Cr_5S_8$[b]	—	—	—	−410	4.04	This work
$TlCr_5S_8$[c]	—	—	15.82	−128	1.21	This work
$Tl_{0.7}Cr_5S_8$[c]	—	—	6.665	−256	2.99	This work

Results of the Fitting Procedure Using Eq. [1] (see text).

	J[cm^{-1}]	g	χ (TIP) (10^{-4} emu/mol)	C (emu K/mol)	Θ(K)	p
$TlCr_5S_8$	−58(2)	1.6(1)	−8.5(1)	1.84	−137(6)	0.8
$Tl_{0.7}Cr_5S_8$	−78(1)	2.4(1)	−31(1)	4.6	−401(24)	0.45

[a] The data of selected Cr chalcogenides are also listed.
[b] Curie–Weiss law.
[c] TIP and Curie–Weiss law (see text).

TABLE 5
Binding Energies (eV) for Thallium, Chromium, and Sulfur in Selected Compounds

Tl	$4f_{5/2}$	$4f_{7/2}$	δ	Ref.
Tl_3VS_4	124.70	120.25	4.45	(31)
Tl_3NbS_4	124.90	120.45	4.45	(31)
Tl_2WS_4	125.1	120.65	4.45	(31)
TlF	126.4	122.0	4.4	(32)
$TlIO_3$	126.3	121.85	4.45	(32)
Tl_2O_3	122.95	118.60	4.35	(32)
Tl	122.2	117.8	4.4	(33)
Tl	122.17	117.73	4.44	(34)
TlV_5S_8	122.6	118.2	4.4	(26)
$Tl_{0.3}V_5S_8$		119.2		(26)
$Tl_{0.8}V_6S_8$		118.1		(35)
$Tl_{0.03}V_6S_8$		119.6		(35)
$TlCr_5S_8$	123.2	118.75	4.45	This work

S	$2p_{3/2}$	Ref.	Cr	$2p_{3/2}$	Ref.
$V_{0.92}S$	162.0	(36)	$CdCr_2S_4$	575.5	(38)
TiS	162.3	(37)	CrS	575.6	(21)
MgS	160.8	(37)	Cr_2S_3	574.8	(40)
GaS	161.0	(37)	Cr_2O_3	576.7	(39)
CrS	161.7	(21)	$CrCl_3$	577.4	(40)
FeS	161.6	(21)	$CrBr_3$	577.4	(40)
NiS	161.7	(21)	CrI_3	576.7	(40)
$TlCr_5S_8$	161.8	This work	CrO_3	579.1	(41)
			Cr	574	(42)
			$TlCr_5S_8$	575.3	This work

It is noteworthy that the gross features between 0 and 10 eV b.e. of the valence band spectra are quite similar to those of the semiconducting monosulfide CrS (21) recorded with AlK_α radiation. The differences of the peak intensities are due to the different cross sections of XPS and He I/He II radiation and the presence of the Tl 6*p* and Tl 6*s* states, respectively (22). The assignment of the not-well-resolved peaks may be the same as for CrS. Chromium 3*d* bands due to different final states are located at 1.3 and 2.9 eV below E_F. The broad features at 4.4 and 6.2 eV are predominantly caused by S 3*p* states which are heavily broadened due to a mixing with Cr 3*d* and Tl 6*s* states. The peak around 10 eV is assigned to a lower state of the S 3*p* valence state. The Tl 5*d* shallow core level is not a sharp simple doublet as observed in the pure Tl metal or in ionic Tl compounds (23) but rather asymmetrical to higher b.e. and significantly broadened. This is an indication for pronounced covalent interactions between the Tl atoms and the Cr_5S_8 host lattice.

3.3.2 The Cr 2p region. The Cr $2p_{3/2}$ and $2p_{1/2}$ core level spectra are displayed in Fig. 5. Reference lines for different Cr compounds are also shown. The observed b.e. of 575.3 eV is of the order reported for other binary and ternary chromium sulfides and selenides, and clearly lower than in oxides or halides (see Table 5). If a linear relationship between core level shift and oxidation state is assumed, the small shift of the core level relative to elemental Cr suggests that the Cr atoms are in an oxidation state far below +3. The spin–orbit coupling of 9.5 eV is also in agreement with the values published for other Cr sulfides/selenides.

The spectrum is highly asymmetrical and background correction according to the Shirley model is difficult due to a too-high background at the high b.e. side. This and the FWHM of 5.7 eV compared to that of Cr_2O_3 with 3.4 eV is indicative of pronounced shake-up structures. Possible multiplet splitting effects are expected to be less pronounced due to the differences in energy between core hole and valence band. These observations point to a highly covalent nature of the compound. Thus the assignment of a formal oxidation state of +3 to the Cr in this compound is of little relevance for the actual bonding situation.

3.3.3 The S 2p region. The S 2*p* core level, together with the b.e. for other sulfur containing substances, is

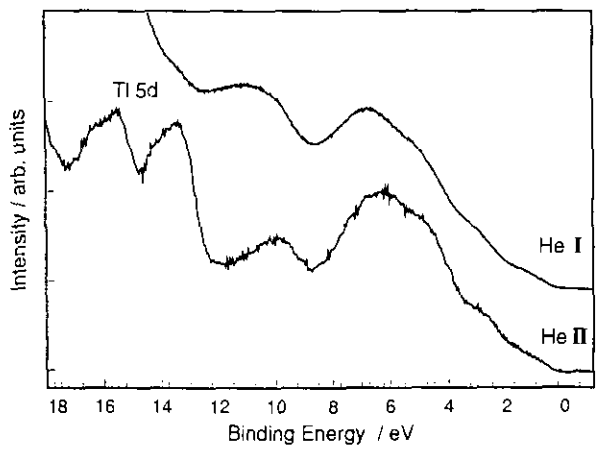

FIG. 4. The valence band UP-spectra (He I and He II) of $TlCr_5S_8$. Note the strong asymmetrical shape of the Tl 5*d* emission.

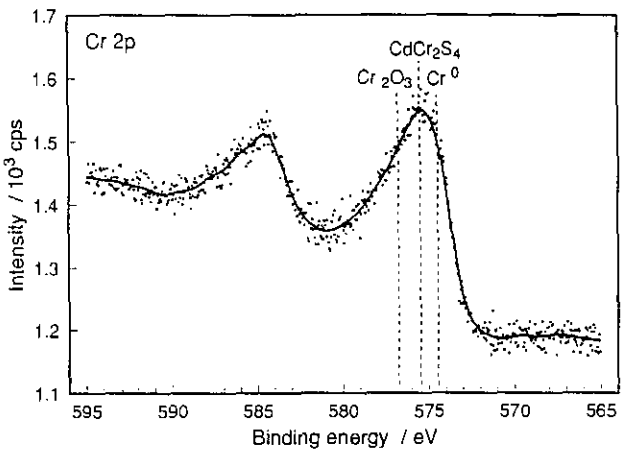

FIG. 5. The XPS Cr 2*p* region of $TlCr_5S_8$. Reference lines for different Cr compounds are given for comparison.

displayed in Fig. 6. The b.e. of 161.8 eV is typical for transition metal sulfides (see Table 5). If a linear relationship between chemical shift and formal oxidation state is again assumed, the small shift compared to elemental sulfur indicates that the formal charge on the sulfur atoms is about -1. The peak is asymmetrical toward the high b.e. side and the S $2p_{1/2}$ is hidden under the peak. The width of the core level of about 2.5 eV gives no indication for the presence of more than one S species.

It should be noted that the asymmetry may also be due to a core hole coupling with delocalized valence electrons (24). Pronounced tails on the S $2p$ signals have been observed in copper sulfides (24, 25) which are metallic. Hence, such tails indicate that the Fermi level in metallic compounds lies in the S $3p$ band (24, 25). Because $TlCr_5S_8$ is a semiconductor, this explanation for the asymmetry can be excluded. Not excludable, however, is the coupling with more localized valence states, i.e., with the shake-up structure seen in the Cr $2p$ spectrum which would be in agreement with the "low" formal oxidation state. Again, this core level spectrum shows clear signs of the high degree of covalent interactions.

At higher b.e., a second peak is observed with an intensity of less than 10% of the main peak at 161.8 eV. Due to the b.e. of 168.8 eV, it is assigned to sulphate species presumably arising from the short exposure to air.

3.3.4 The Tl 4f core level. The thallium 4 $f_{5/2}$ and 4 $f_{7/2}$ core level lines are shown in Fig. 7. Reference lines for elemental Tl, TlV_5S_8, and Tl_3VS_4 are also displayed (compare also Table 5). The line shape of the Tl $4f$ core level is different from a purely metallic system as a consequence of the different core hole coupling in the two systems $TlCr_5S_8$ without delocalized valence electrons and thallium metal with the delocalized valence electrons. The b.e. for the 4 $f_{5/2}$ and 4 $f_{7/2}$ core levels are 123.2 and 118.75 eV, respectively, with a spin-orbit coupling of 4.45 eV which is nearly identical with the values obtained for

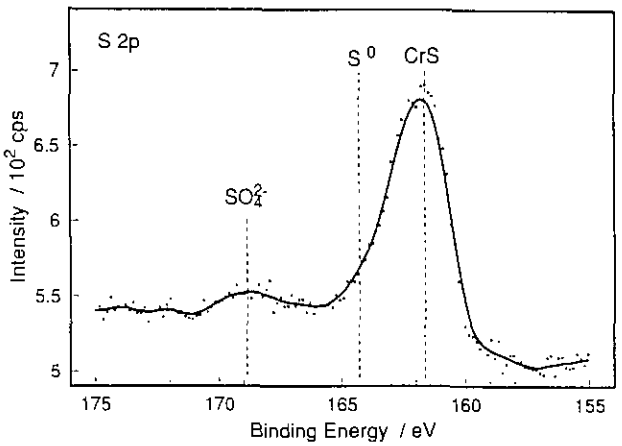

FIG. 6. The XPS S $2p$ region of $TlCr_5S_8$. Reference lines for different S compounds are given for comparison.

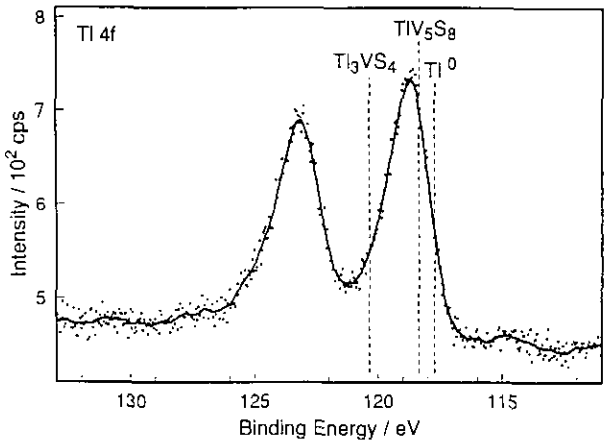

FIG. 7. The XPS Tl $4f$ region of $TlCr_5S_8$. Reference lines for different Tl compounds are given for comparison.

TlV_5S_8 (26) but lower than the values observed for ternary compounds such as Tl_3NbS_4 and Tl_3VS_4 (see Table 5). These compounds are, however, structurally different and contain isolated Tl ions located between MS_4 tetrahedra. A comparison with more ionic compounds like TlF suggests that the Tl atoms carry only a small positive charge and are in an oxidation state clearly below $+1$. The FWHM of about 1.8 eV is slightly larger than in elemental Tl (22).

4. CONCLUSIONS

$TlCr_5S_8$ is isotypic with TlV_5S_8. In contrast to the V compound the Cr–Cr interatomic distances are inequivalently distributed and suggest the formation of "isolated" Cr_2-dimers rather than an infinite two-dimensional metal atom network as observed in the V compound. In addition, the environment of the Tl atoms is more asymmetrical than in the V compound and may be described as a 4 + 6 coordination. The magnetic behavior of $TlCr_5S_8$ and $Tl_{0.7}Cr_5S_8$ is complex and indicative for low-dimensional magnetic systems. The two compounds exhibit significant differences of the temperature dependence of the susceptibility. These differences suggest appreciable changes of the Cr–Cr interatomic interactions as a function of Tl content. For both samples the most successful model to describe the magnetic properties considers the crystal structure as composed of isolated Cr_2-dimers and isolated Cr atoms. With decreasing Tl concentration, the Curie–Weiss-like contribution to the susceptibility increases and the evaluated values for the coupling constant J as well as for the Weiss contant Θ point to stronger antiferromagnetic interactions in the Tl-poor sample. In the isotypic compound $Tl_xV_5S_8$ the V2–V3 distance increases by about 0.2%, whereas the V1–V3 and V2–V2 separations decrease by 0.6% and 0.5%, respectively, when the Tl content is lowered to $x = 0.70$. Assuming

similar changes of the metal to metal distances as a function of the Tl content in the $Tl_xCr_5S_8$ system, the interatomic separation within the Cr_2 pairs increases with decreasing Tl abundance and the interatomic distances between the Cr2 atoms of the pairs and the Cr3 atoms of the pairs and the isolated Cr1 atom decrease. Attempts to explain the magnetic properties with a simple Curie–Weiss law or with a Curie–Weiss law and a contribution of a temperature independent Pauli-paramagnetism were less successful. In summary, the magnetic behavior of the two compounds is not fully understood.

UPS investigations of the valence band region reveal that $TlCr_5S_8$ is a semiconductor. This conclusion is further supported by electrical resistivity measurements performed on a pressed powder pellet. The valence band region is dominated by S 3*p* and Cr 3*d* states and broadened due to the hybridization with Tl 6*s* and 6*p* states. The observed binding energies of the core level lines of Tl, Cr, and S, as well as the shape of the emission peaks, are indicative for low formal charges on these atoms. The interaction between the Tl atoms and the Cr_5S_8 host matrix and the interactions within the host matrix are highly covalent.

ACKNOWLEDGMENTS

Helpful discussions with Professor Schlögl and with Dr. F. Tuzcek (University of Mainz) as well as financial support by the Deutsche Forschungsgemeinschaft (DFG) are gratefully acknowledged.

REFERENCES

1. L. Fournes, M. Vlasse, and M. Saux, *Mater. Res. Bull.* **12,** 1 (1977).
2. J. Huster, *Z. Kristallogr.* **144,** 146 (1979).
3. J. Huster, *Z. Anorg. Allg. Chem.* **447,** 89 (1978).
4. N.-H. Dung, V.-V. Tien, H. J. Behm, and P. T. Beurskens, *Acta Crystallogr. Sect. C* **43,** 2258 (1987).
5. T. Ohtani and S. Onoue, *Mater. Res. Bull.* **21,** 69 (1986).
6. K. D. Bronsema, J. Mahy, *Phys. Status Solidi A* **104,** 603 (1987).
7. K. D. Bronsema, R. Jansen, and G. A. Wiegers, *Mater. Res. Bull.* **19,** 555 (1984).
8. R. Quint and H. Boller, *Mater. Res. Bull.* **22,** 1499 (1987).
9. K. Klepp and H. Boller, *J. Solid State Chem.* **48,** 388 (1983).
10. W. Bensch, K. Polborn, E. Amberger, W. Steurer, and J. Abart, *J. Solid State Chem.* **55,** 121 (1984).
11. W. Bensch, E. Amberger, and J. Abart, *Solid State Commun.* **51,** 979 (1984).
12. M. Rosenberg, A. Knülle, H. Sabrowsky, and C. Platte, *J. Phys. Chem. Solids* **43,** 87 (1982).
13. K. Vidyasagar and J. Gopalakrishnan, *J. Solid State Chem.* **42,** 217 (1982).
14. H. Lueken and W. Rohne, *Z. Anorg. Allg. Chem.* **418,** 103 (1975).
15. C. D. Wagner, L. E. Davis, M. V. Zeller, J. A. Taylor, R. M. Raymond, and L. H. Gale, *Surf. Interface Anal.* **3,** 211 (1981).
16. W. Bensch and E. Wörner, *Solid State Ionics* **58,** 275 (1992).
17. R. J. Bouchard, P. A. Russo, and A. Wold, *Inorg. Chem.* **4,** 685 (1965).
18. W. Bronger, *Ber. Bunsenges, Phys. Chem.* **96,** 1372 (1992).
19. C. J. O'Connor, *Prog. Inorg. Chem.* **29,** 203 (1982).
20. W. Bensch and E. Wörner, in press.
21. A. Gopalakrishnan, T. Murugesan, M. S. Hedge, and C. N. R. Rao, *J. Phys. C.* **12,** 5255 (1979).
22. R. Schlögl, V. Geiser, P. Oelhafen, and H.-H. Güntherodt, *Phys. Rev. B* **35,** 6414 (1987).
23. R. Schlögl, V. Geiser, and P. Oelhafen, "MRS Proceedings," E-207. Boston, 1987.
24. J. C. W. Folmer and D. K. G. deBoer, *Solid State Commun.* **38,** 1135 (1981).
25. J. C. W. Folmer and F. Jellinek, *J. Less-Common Met.* **76,** 153 (1980).
26. W. Bensch, E. Wörner, U. Ruschewitz, and M. Muhler, *Eur. J. Solid State Inorg. Chem.* **30,** 645 (1993).
27. Y. Tazuke, *J. Phys. Soc. Jpn.* **50,** 413 (1981).
28. A. Hayashi, Y. Ueda, K. Kosuge, H. Murata, A. Asano, and N. Watanabe, *J. Solid State Chem.* **67,** 346 (1987).
29. D. Babot, M. Wintenberger, B. Lambert-Andron, and M. Chevreton, *J. Solid State Chem.* **8,** 175 (1973).
30. A. W. Sleight and T. A. Bither, *Inorg. Chem.* **8,** 566 (1969).
31. A. Müller, Ch. K. Jörgensen, and E. Diemann, *Z. Anorg. Allg. Chem.* **391,** 38 (1972).
32. Ch. K. Jörgensen, *Theor. Chim. Acta* **24,** 241 (1972).
33. J. C. Fuggle and N. Martensson, *J. Electron Spectrosc. Relat. Phenom.* **21,** 275 (1980).
34. N. Martensson, A. Berndtson, and R. Nyholm, *J. Electron Spectrosc. Relat. Phenom.* **19,** 299 (1980).
35. W. Bensch, J. Koy, and M. Wesemann, *J. Alloys Compounds* **178,** 193 (1992).
36. H. F. Franzen and G. A. Sawatzky, *J. Solid State Chem.* **15,** 229 (1975).
37. J. Nakahara, H. F. Franzen, and D. K. Misemer, *J. Chem. Phys.* **76,** 4080 (1982).
38. C. Battistoni, E. Paparazzo, Y. Dumond, and M. Nogues, *Solid State Commun.* **46,** 333 (1983).
39. D. Shuttleworth, *J. Phys. Chem.* **84,** 1629 (1980).
40. J. C. Carver, G. K. Schweitzer, and T. A. Carlson, *J. Chem. Phys.* **57,** 973 (1972).
41. R. Merryfield, M. McDaniel, and G. Parks, *J. Catal.* **77,** 348 (1982).
42. J. A. Lezo and E. E. Minni, *Philos. Mag. B* **49,** L61 (1984).